Proceedings of the 2025 SICE Festival with Annual Conference
September 9-12, 2025, Chiang Mai, Thailand

Local Planning for an Autonomous Mobile Robot to Reduce Pedestrian Uncertainty

Aiki Kada[1†], Kohei Honda[1], Hiroyuki Okuda[1], and Tatsuya Suzuki[1]

[1]Department of Mechanical System Engineering, University of Nagoya, Aichi, Japan
(Tel: +81-52-789-2700; E-mail: kada.aiki.u3@s.mail.nagoya-u.ac.jp)

Abstract: This paper proposes a novel local planning approach for Autonomous Mobile Robots (AMRs) to reduce pedestrian uncertainty during human-robot interactions in shared spaces. We introduce a quantitative measure of pedestrian uncertainty through a "decision entropy" framework that captures the uncertainty in crossing-order decisions. While existing research has focused primarily on predicting pedestrian physical movements, our method addresses the cognitive aspects of decision-making processes during robot-human encounters. By simultaneously optimizing both linear and angular velocities, our controller minimizes pedestrian uncertainty and creates more predictable robot behaviors. We extend previous decision entropy concepts to incorporate rotational movements, enabling the robot to clearly communicate its intentions through deliberate motion patterns. Experimental validation in real-world crossing scenarios demonstrates that our approach significantly reduces uncertainty metrics when the AMR follows pedestrians, resulting in more decisive interactions and improved pedestrian comfort. This work establishes a foundation for developing socially-aware navigation systems that consider pedestrian psychological responses in shared environments.

Keywords: Human-Machine Systems; Robotic and Automation Systems; Modeling, System Identification and Estimation

1. INTRODUCTION

Autonomous Mobile Robots (AMRs) have gained significant traction across logistics warehouses, manufacturing facilities, and service industries as solutions to labor shortages and operational efficiency challenges. The deployment of AMRs in human-shared environments has attracted considerable attention in industrial applications due to their versatility and adaptability. In such contexts, AMRs must respond appropriately not only to static obstacles but also to dynamic and unpredictable agents such as humans [1].

One of the primary challenges in human-robot shared scenarios is the uncertainty in mutual intention understanding. This uncertainty causes the Freezing Robot Problem (FRP), where robots become overly cautious or stop in crowded environments [2]. As Trautman et al. demonstrated, even perfect prediction cannot solve FRP without understanding natural human collision avoidance [3]. Following Sathyamoorthy et al. approach of avoiding freezing zones [4], proactive uncertainty reduction could guide interactions toward more predictable situations. In addition, this 'uncertainty' is more than just an inefficient; it affects the perceived reliability and acceptability of robots, ultimately becoming a critical factor determining the successful adoption of AMR systems. Dragan et al. [5] demonstrated that in human-robot collaboration with manipulators, robot motion designed to clearly express intentions ('legible motion') reduced coordination time by 33% compared to merely predictable motion. While their work focused on robotic arms in collaborative tasks, this principle of motion legibility is equally critical for AMRs navigating in shared spaces. Recent research by Hetherington et al. [6] further reinforces this notion, showing that pedestrians encountering mobile robots without clear communication of movement intentions experience significant discomfort, confusion, and delayed social acceptance.

Traditional research on AMR motion planning has predominantly focused on safety and efficiency aspects. Approaches such as the Social Force Model (SFM) [7, 8], Reciprocal Velocity Obstacles (RVO) [9], and Optimal Reciprocal Collision Avoidance (ORCA) [10] excel at physical collision avoidance but insufficiently address the psychological aspects of pedestrian behavior, particularly the uncertainty in decision-making processes. Similarly, studies employing deep reinforcement learning [11, 12] and imitation learning [13, 14] have became a common approach, but these studies concentrate on predicting pedestrian physical movements with limited consideration of cognitive aspects.

Okuda et al. [15] introduced the concept of 'decision entropy' in vehicle-to-vehicle interactions for autonomous driving, achieving smooth merging coordination by quantifying uncertainty in other drivers' decisions. While groundbreaking in considering decision-making uncertainty, this approach was developed for environments constrained by lanes, limiting interactions primarily to velocity control.

Several researches have attempted to apply similar decision entropy concepts to AMR navigation [16, 17]. However, these adaptations have also primarily focused on linear velocity control as the main parameter for reducing uncertainty, inheriting the same limitations as the original automotive applications. Conversely, the environments where AMRs operate, such as sidewalks and indoor corridors, are shared spaces with fewer constraints than roadways, and pedestrians are in closer proximity. Consequently, not only the robot's linear velocity but

† Aiki Kada is the presenter of this paper.

also its turning behavior and direction of travel significantly impact interactions with pedestrians. This multi-dimensional aspect of AMR motion planning for uncertainty reduction remains largely unexplored in previous research.

This study proposes a control method that achieves smoother human-robot interactions by reducing pedestrian 'uncertainty' in two-dimensional operational space. First, we analyze how rotational behavior affects decision entropy in human-robot interactions. Next, we develop a control method that simultaneously optimizes both linear and angular velocities to minimize uncertainty. Specifically, we extend the decision entropy framework, which quantifies uncertainty, to incorporate angular velocity considerations, and implement a behavior planning strategy that minimizes pedestrian uncertainty through simultaneous control of both velocity components. We validate the effectiveness of the proposed method through comprehensive real-world experiments comparing our approach against conventional control strategies.This paper has two significant contributions:

1. Analysis and quantification of uncertainty metrics incorporating rotational behavior of robots, and evaluation of the effect of the rotation on the decision uncertainty of human.
2. Development of a decision entropy minimization technique that integrates both linear and angular velocities

These contributions extend beyond efficient collision avoidance to enhance the social acceptability of AMRs through human-centered design principles, addressing a critical gap in existing navigation methodologies for shared human-robot environments.

2. PROBLEM SETTING

Human-robot shared environments present a diverse range of interaction scenarios that vary significantly in complexity and context [18]. In such environments, AMRs must navigate while considering not only static obstacles but also the dynamic and often unpredictable behavior of pedestrians. These scenarios differ widely based on pedestrian density, spatial configurations, environmental constraints, and cultural factors, creating a complex problem space for robot navigation systems.

We focus on a fundamental scenario: an AMR and pedestrian approaching at vertical angles. This common indoor interaction pattern captures the essential challenge of mutual intention understanding.

In these crossing situations, both the robot and pedestrian see each other and communicate without words by changing their speed and turning to avoid collisions. The pedestrian must decide whether to let the robot go first or to proceed first, based on limited information about what the robot plans to do. This decision-making process varies greatly between different pedestrians and situations, often creating uncertainty that shows up as changes in speed, path changes, or brief stops. This uncertainty not only makes movement less smooth and efficient but also makes pedestrians uncomfortable and less accepting of robots in shared spaces.

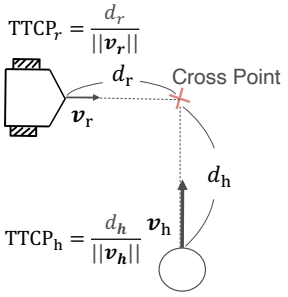

Fig. 1: Illustration of Time To Cross Point (TTCP) calculation for both the pedestrian and AMR. TTCP is defined as the ratio between distance to crossing point (d_h, d_r) and magnitude of velocity vectors ($\|v_h\|$, $\|v_r\|$).

Our approach adjusts both linear and angular velocities to reduce pedestrian uncertainty, creating smoother interactions beyond collision avoidance by modeling decision uncertainty.

3. PROPOSED METHOD

3.1. Quantification of uncertainty

In this study, we define uncertainty as the lack of clarity about who goes first during perpendicular crossing interactions. When pedestrians and AMRs meet at crossing points, pedestrians feel discomfort when it is not clear who should cross first. To measure this uncertainty in a number-based way, we create a probability model that looks at the differences in crossing times.

3.1.1. Modeling the pedestrian's ahead probability

First, we introduce the Time To Cross Point (TTCP). We could use many different models to understand how pedestrians decide in crossing situations (such as models based on speed changes, personal space, or where pedestrians look [18]), but we choose a simpler approach using TTCP as main explanatory variable because it is easy to understand and calculate. Let $\text{TTCP}_\text{h}(t)$ and $\text{TTCP}_\text{r}(t)$ represent the TTCP of the pedestrian and AMR at time t, which are calculated as follows:

$$\text{TTCP}_\text{h}(t) = \frac{d_\text{h}(t)}{\|\boldsymbol{v}_\text{h}(t)\|} \tag{1}$$

$$\text{TTCP}_\text{r}(t) = \frac{d_\text{r}(t)}{\|\boldsymbol{v}_\text{r}(t)\|} \tag{2}$$

where $d_\text{h}(t)$ and $d_\text{r}(t)$ represent the distances to the crossing point for the pedestrian and AMR, and $\boldsymbol{v}_\text{h}(t)$ and $\boldsymbol{v}_\text{r}(t)$ are their respective velocity vectors, as illustrated in Fig. 1.

Using the difference in TTCP, defined as $\Delta\text{TTCP}(t) = \text{TTCP}_\text{r}(t) - \text{TTCP}_\text{h}(t)$, as the primary explanatory variable, we model the probability P of the pedestrian deciding to cross first through logistic regression:

$$P(t) = \frac{1}{1 + \exp(-(\eta_1 + \eta_2 \Delta\text{TTCP}(t)))} \tag{3}$$

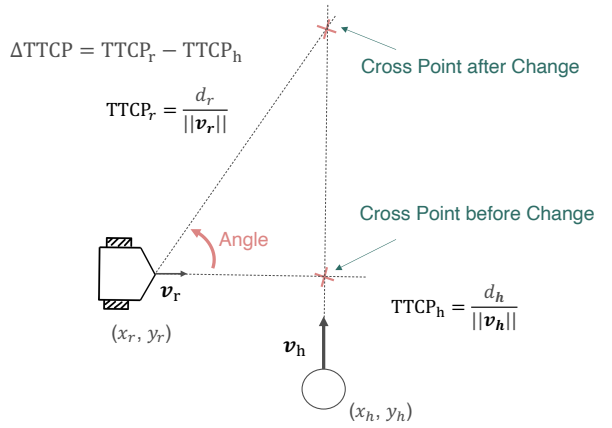

Fig. 2: Schematic representation of AMR's rotational effect on the crossing scenario. The AMR rotates in the positive direction (counterclockwise, toward the pedestrian's front path) in this configuration.

where η_1 and η_2 are model parameters identified from experimental data. This probability model approaches 1 when $\text{TTCP}_\text{r}(t) - \text{TTCP}_\text{h}(t) \gg 0$ (AMR's arrival is clearly later) and approaches 0 when $\text{TTCP}_\text{r}(t) - \text{TTCP}_\text{h}(t) \ll 0$ (AMR's arrival is clearly earlier).

3.1.2. Uncertainty Metric: Decision Entropy

To quantify pedestrian uncertainty, we define the decision entropy $S(t)$ based on probability $P(t)$ using Shannon's information entropy:

$$S(t) = -P(t)\log P(t) - (1 - P(t))\log(1 - P(t)) \quad (4)$$

This decision entropy $S(t)$ has the following characteristics:

- When $P(t)$ is close to 0 or 1 (clear crossing order): $S(t)$ approaches 0
- When $P(t)$ is close to 0.5 (ambiguous crossing order): $S(t)$ approaches 1

3.1.3. Effect of AMR's angular velocity

We simulate how the AMR's rotation affects the measured uncertainty (decision entropy) as defined in Equation 4 before using decision entropy for the controller. Different interaction models would show different relationships between robot actions and pedestrian uncertainty. In our approach, we use the TTCP-based probability model to analyze these effects. Consider a situation with starting positions at $x_r = 0$, $y_r = 0$, $x_h = 5.0$, and $y_h = 5.0$, where the AMR rotates in the positive direction (clockwise, toward the pedestrian's front path) as illustrated in Fig. 2. The resulting changes in ΔTTCP and the pedestrian's ahead probability with respect to the AMR's rotation angle are shown in the following figures.

Fig. 3 illustrates how the ΔTTCP (=TTCP$_r$ - TTCP$_h$) varies with the AMR's rotation angle at different AMR speeds. We observe that as the rotation angle increases in the positive direction, ΔTTCP generally decreases,

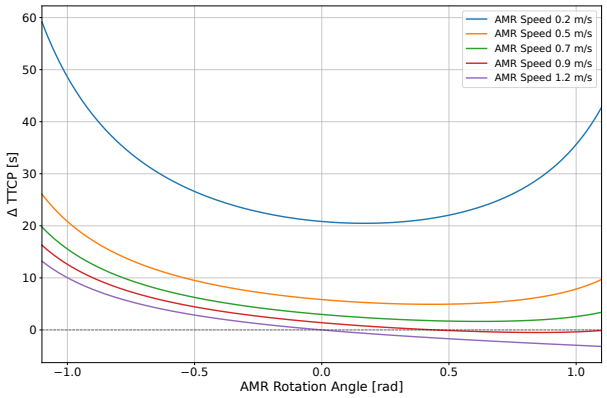

Fig. 3: Effect of AMR's rotation angle on ΔTTCP (TTCP$_r$ - TTCP$_h$) at different AMR speeds.

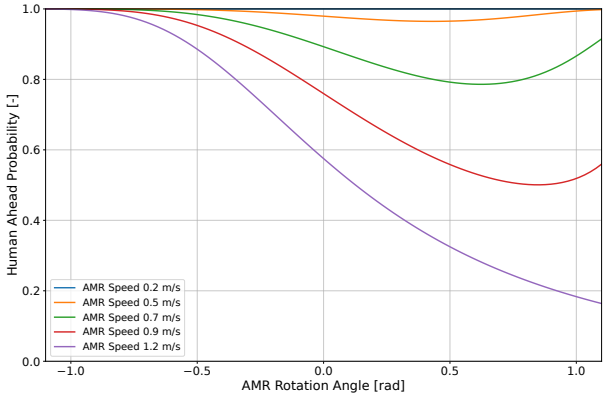

Fig. 4: Effect of AMR's rotation angle on the pedestrian's ahead probability at different AMR speeds.

indicating that the AMR would arrive at the crossing point earlier relative to the pedestrian. Conversely, negative rotation angles tend to increase ΔTTCP, suggesting the AMR would arrive later than the pedestrian. This relationship becomes more pronounced at higher AMR speeds.

As shown in Fig. 4, when the AMR's rotation angle is between about -1 and 1 radians, the probability of the pedestrian going ahead decreases when the AMR turns more in the positive direction, and increases when the AMR turns more in the negative direction. This means that when the AMR turns to pass in front of the pedestrian, the pedestrian is less likely to go ahead, and when the AMR turns to pass behind the pedestrian, the pedestrian is more likely to go ahead. This behavior is similar to what we usually see in human-human interactions, where pedestrians who go first tend to pass in front of others, while those who go second tend to pass behind others. So, our ahead probability model defined in Equation 3 seems to correctly respond to changes in the AMR's rotating behavior as well. Fig. 5 demonstrates how decision entropy changes with the AMR's rotation angle. These results confirm that uncertainty can be significantly modulated not only through velocity adjustments but also through rotational movements. The decision entropy ex-

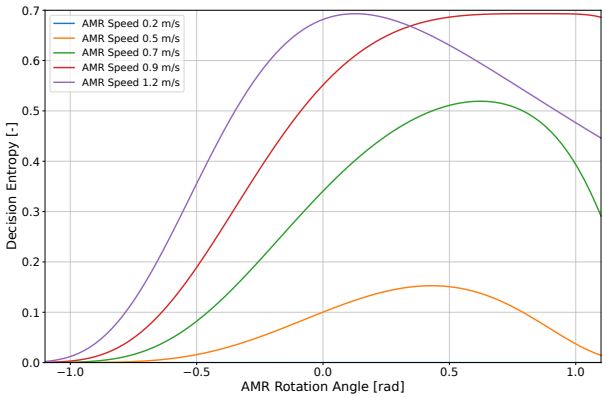

Fig. 5: Effect of AMR's rotation angle on decision entropy at different AMR speeds.

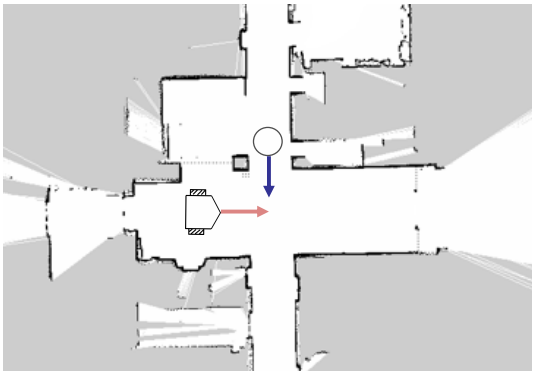

Fig. 6: Experimental environment for the orthogonal crossing scenario between an AMR and a pedestrian.

hibits different patterns depending on both the AMR's speed and rotation angle, suggesting that the combination of these control parameters offers greater flexibility in reducing pedestrian uncertainty during crossing interactions.

3.2. Motion Planning to Reduce Uncertainty of Pedestrian's Decision

In this study, Model Predictive Path Integral control (MPPI) is exploited to solve the optimal control problem. MPPI combines optimal control theory with sampling-based stochastic optimization, making it effective for complex systems with nonlinearities and constraints. As shown in Equation (5), our objective is to minimize the expected value of the cost function:

$$\boldsymbol{E}_{\boldsymbol{u}\sim q}\left[\sum_{k=0}^{N-1} L(\boldsymbol{x}(k|t),\boldsymbol{u}(k|t))\right] \tag{5}$$

where q represents the sampling distribution of control inputs and N denotes the prediction horizon length. The cost function L comprises multiple terms as defined in Equation (6):

$$\begin{aligned} L(\boldsymbol{x}(k|t),\boldsymbol{u}(k|t)) =& w_1\|\boldsymbol{x}_{\mathrm{r}}^{\mathrm{ref}} - \boldsymbol{x}_{\mathrm{r}}(k|t)\| \\ &+ w_2\|\boldsymbol{v}_{\mathrm{r}}^{\mathrm{ref}} - \boldsymbol{v}_{\mathrm{r}}(k|t)\| \\ &+ w_3\delta_1{}^{-\|\boldsymbol{x}_{\mathrm{r}}(k|t)-\boldsymbol{x}_{\mathrm{h}}(k|t)\|} \\ &+ w_4 S(k|t) \end{aligned} \tag{6}$$

The first term punishes differences from the target position, while the second term punishes differences from the target speed. The third term keeps safety by making the cost increase quickly as the distance between the AMR and pedestrian gets smaller. The fourth term includes the decision entropy $S(k|t)$, which is the core contribution of this work for minimizing pedestrian uncertainty. The weighting coefficients w_1 through w_4 are adjusted based on system needs and desired performance characteristics.

In the MPPI algorithm, we sample control input candidates and predict the system's behavior using these inputs. The AMR dynamics are modeled by Equations (7)-(10):

$$\boldsymbol{x}_r(k+1|t) = \boldsymbol{x}_r(k|t) + \boldsymbol{v}_r(k|t)\Delta t \tag{7}$$
$$\theta_r(k+1|t) = \theta_r(k|t) + \omega_r(k|t)\Delta t \tag{8}$$
$$\boldsymbol{v}_r(k+1|t) = \boldsymbol{v}_r(k|t)R(\theta(k|t)) \tag{9}$$
$$R(\theta) = \begin{bmatrix}\cos\theta & -\sin\theta \\ \sin\theta & \cos\theta\end{bmatrix} \tag{10}$$

where $\boldsymbol{x}_r$ represents the AMR position, θ_r is the orientation angle, $\boldsymbol{v}_r$ is the velocity vector, and ω_r is the angular velocity. The rotation matrix $R(\theta)$ updates the velocity vector based on the AMR's orientation.

The pedestrian model is described by Equations (11)-(14). An important feature is that the pedestrian's maximum and minimum speeds change dynamically based on the probability $P(t)$

$$v_{\mathrm{h}}^{\max}(t) = v(0|t) + v_{\mathrm{h}}^{\mathrm{diff}} \cdot P(0|t) \tag{11}$$
$$v_{\mathrm{h}}^{\min}(t) = v(0|t) - v_{\mathrm{h}}^{\mathrm{diff}} \cdot (1 - P(0|t)) \tag{12}$$

Additionally, we use a model where the pedestrian's direction stays the same while only the speed changes:

$$\|\boldsymbol{v}_{\mathrm{h}}(k+1|t)\| = v_{\mathrm{h}}^{\max} \cdot P(k|t) + v_{\mathrm{h}}^{\min} \cdot (1 - P(k|t)) \tag{13}$$

$$\boldsymbol{v}_{\mathrm{h}}(k+1|t) = \|\boldsymbol{v}_{\mathrm{h}}(k+1|t)\| \cdot \frac{\boldsymbol{v}_{\mathrm{h}}(k|t)}{\|\boldsymbol{v}_{\mathrm{h}}(k|t)\|} \tag{14}$$

In the MPPI framework, we evaluate the cost function for each control input candidate and find the best control input by weighted averaging. This process is repeated at each time step, enabling adaptive control in dynamically changing environments. Specifically, our approach optimizes both linear and angular velocities at the same time, which effectively reduces pedestrian uncertainty during interactions.

4. EXPERIMENT

4.1. Experiment Setup

We implemented the proposed control method on a physical system and experimentally validated an vertical

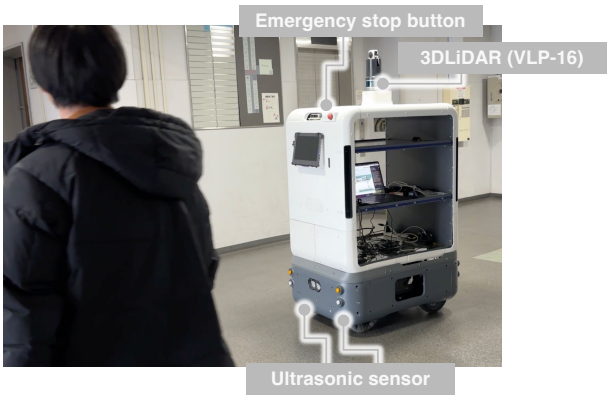

Fig. 7: Hardware configuration of the experimental system.

Table 1: Entropy Term Weight Conditions

Notation	Description
w/o entropy	Experiments with $w_4 = 0.0$ (entropy term disabled)
w/ entropy	Experiments with $w_4 = 5.0$ (entropy term enabled)

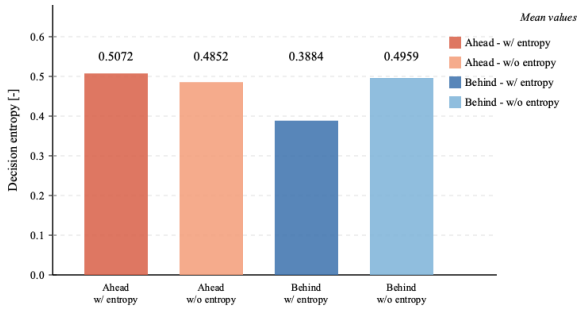

Fig. 8: Comparison of average decision entropy values between the proposed method (w/ entropy) and conventional method (w/o entropy) in both Ahead and Behind scenarios.

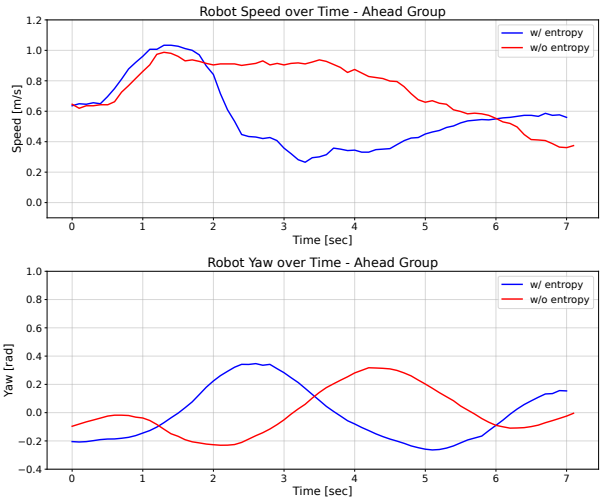

Fig. 9: Comparison of speed and yaw angle profiles over time in the Ahead scenario.

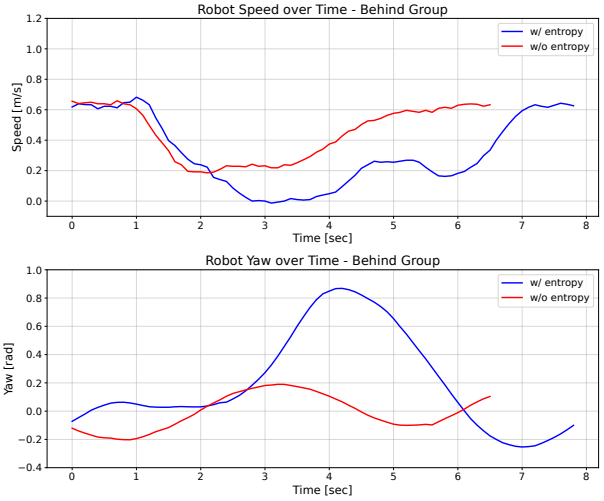

Fig. 10: Comparison of speed and yaw angle profiles over time in the Behind scenario.

crossing scenario between one AMR and one pedestrian. The experimental environment consisted of a 6-meter wide corridor intersection, with measurements taken approximately 5 meters before and after the intersection point.

The experimental conditions are shown in Table 1, comparing scenarios with and without the entropy term (uncertainty reduction term) from Equation (6). We conducted experiments with the weight parameter w_4 set to 0.0 (without entropy term) and 5.0 (with entropy term). The measurement began when the AMR detected the pedestrian and ended when both agents completely passed each other (when their respective TTCP values became negative)

4.2. Results

As shown in Fig. 8, the average decision entropy value was reduced by the proposed method (w/ entropy) when the AMR was following the pedestrian (Behind scenario). In contrast, when the AMR was leading and the pedestrian was following (Ahead scenario), no significant difference in decision entropy values was observed between the proposed method (w/ entropy) and the conventional method (w/o entropy).

Fig. 9 through 12 show the temporal profiles of speed, yaw angle, and decision entropy in both the Ahead and Behind scenarios. In the Ahead scenario (AMR leading), the speed profile with the entropy term shows more distinctive motion patterns, with sharp acceleration followed by clear deceleration, demonstrating more decisive movement.

In the Behind scenario (pedestrian leading), the conventional method (w/o entropy) shows that the AMR tends to maintain a relatively constant speed around $v = 0.2$ m/s. In contrast, the proposed method (w/ entropy) demonstrates a more significant deceleration, with the

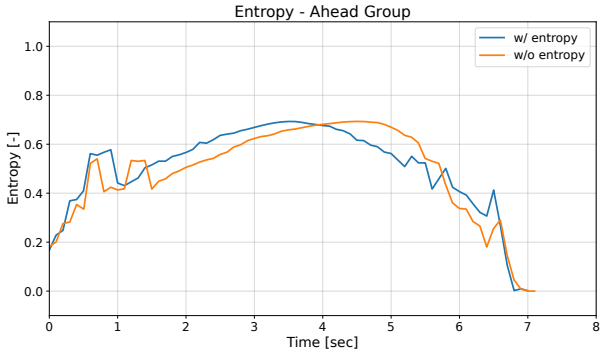

Fig. 11: Comparison of decision entropy profiles over time in the Ahead scenario.

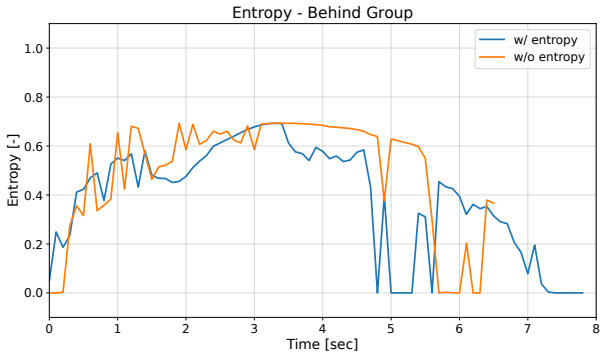

Fig. 12: Comparison of decision entropy profiles over time in the Behind scenario.

speed approaching $v = 0.0$ m/s, indicating a more decisive stopping behavior to solve the potential conflict.

Regarding the yaw angle profiles, no significant difference was observed in the Ahead scenario, with both methods showing minimal rotation within the margin of error. However, in the Behind scenario, the proposed method (w/ entropy) showed a notably larger rotation angle, which represent a characteristic behavior pattern facilitated by the entropy term in the cost function.

These results suggest that the entropy term effectively reduces decision entropy, particularly when the AMR follows the pedestrian, leading to more decisive and communicative motion behaviors that can better convey the robot's intentions during human-robot interactions in crossing scenarios.

5. DISCUSSION

In this study, we proposed a control method for AMRs aimed at reducing pedestrian uncertainty during crossing interactions. Our findings suggest that our proposed approach can reduce uncertainty not only through distinctive speed changes but also through rotational movements.

However, the reduction in decision entropy values was only observed in the Behind scenario (when the AMR followed the pedestrian). We attribute this asymmetric result partly due to the characteristics of our decision entropy function, which changes non-uniformly in relation to the speeds of both the AMR and the pedestrian. Specifically, in our designed function, when the AMR operates at low speeds, yaw angle changes can effectively reduce the cost function value. In contrast, at higher AMR speeds, yaw angle adjustments have minimal impact on reducing the cost function.

Fig. 13 shows this relationship through heatmaps of the entropy function based on the AMR's speed and yaw angle computed from our decision model of the pedestrian. These heatmaps were created with two main assumptions: first, that either the AMR or the pedestrian would give way while the other continues moving; and second, that the combined speed of the AMR and pedestrian would always add up to 1.5 m/sAs shown in Fig. 13(a), the probability map indicates the probability of the pedestrian moving ahead of the AMR.When the probability value is 1, it means the pedestrian is going ahead (moving first before the AMR). Notably, at lower AMR speeds ($v = 0.2$-0.4 m/s), the pedestrian's probability of going first remains consistently high regardless of the AMR's rotation angle. However, as the AMR moves faster, the rotation angle begins to significantly affect the pedestrian's decision.

As shown in Fig. 13(b), when focusing only on reducing entropy, there is little difference in entropy values across different turning angles when the AMR moves slowly ($v = 0.2$-0.4 m/s).

However, the optimal solution comes from the combined effects of multiple terms in the cost function. For instance, when including the speed reference factor (the second term in the cost function) that aims to maintain close to the reference speed ($v = 0.7$ m/s), as shown in Fig. 13(c), the optimal solution tends toward slightly increasing speed while applying a larger positive yaw angle, as depicted in Fig. 13(d). On the other hand, at higher AMR speeds (v = 0.8–1.0 m/s), simply increasing speed appears enough to approach the optimal solution, as shown in Fig. 13(d). These analytical observations match our experimental results. In the Ahead scenario, we saw minimal turning angle changes but clear speed adjustments, while the Behind scenario showed significant turning angle changes along with speed increases.

6. CONCLUSION

Our proposed method suggests that using turning speed (angular velocity) as a control variable could further reduce decision uncertainty in Behind scenarios. However, we have not yet tested whether these reductions in decision entropy actually lead to less uncertainty and discomfort for pedestrians. Future research should include feedback from pedestrians to evaluate if they feel less uncertain and anxious. Also, more research is needed to design better functions that can effectively reduce decision uncertainty in Ahead scenarios too.

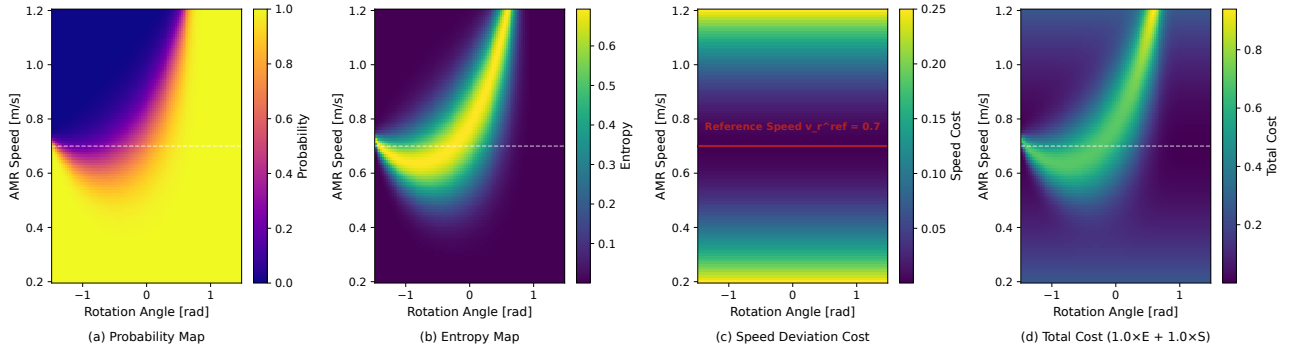

Fig. 13: Heatmaps showing the cost function components with respect to AMR velocity and yaw angle: (a) probability map, (b) entropy map, (c) speed deviation cost, and (d) total cost function.

ACKNOWLEDGMENT

This study was conducted as a joint research project with Toyota Motor Corporation (1 Toyota-cho, Toyota City, Aichi, Japan). We sincerely appreciate the support and contributions of all those involved

REFERENCES

[1] R. Korbmacher and A. Tordeux. Review of pedestrian trajectory prediction methods: Comparing deep learning and knowledge-based approaches. *IEEE Trans. Intelligent Transportation Systems*, 23(12):24126–24144, 2022.

[2] P. Trautman and A. Krause. Unfreezing the robot: Navigation in dense, interacting crowds. In *2010 IEEE/RSJ Int. Conf. Intelligent Robots and Systems*. IEEE, 2010.

[3] P. Trautman, J. Ma, R. M. Murray, and A. Krause. Robot navigation in dense human crowds: Statistical models and experimental studies of human–robot cooperation. *The Int. J. Robotics Research*, 34(3):335–356, 2015.

[4] A. J. Sathyamoorthy, J. Liang, U. Patel, T. Guan, R. Chandra, and D. Manocha. Frozone: Freezing-free, pedestrian-friendly navigation in human crowds. *IEEE Robotics and Automation Letters*, 5(3):4352–4359, 2020.

[5] A. D. Dragan, K. C. T. Lee, and S. S. Srinivasa. Effects of robot motion on human-robot collaboration. In *Proc. the Tenth Annual ACM/IEEE Int. Conf. Human-Robot Interaction*. ACM/IEEE, 2015.

[6] N. J. Hetherington, E. A. Croft, and H. F. M. Van der Loos. Hey robot, which way are you going? Nonverbal motion legibility cues for human-robot spatial interaction. *IEEE Robotics and Automation Letters*, 6(3):5010–5015, July 2021.

[7] D. Helbing and P. Molnar. Social force model for pedestrian dynamics. *Physical Review E*, 51(5):4282, 1995.

[8] G. Ferrer and A. Sanfeliu. Proactive kinodynamic planning using the extended social force model and human motion prediction in urban environments. In *2014 IEEE/RSJ Int. Conf. Intelligent Robots and Systems*, pages 1730–1735. IEEE, 2014.

[9] J. van den Berg, M. Lin, and D. Manocha. Reciprocal velocity obstacles for real-time multi-agent navigation. In *2008 IEEE Int. Conf. Robotics and Automation*. IEEE, 2008.

[10] J. van den Berg, S. J. Guy, M. Lin, and D. Manocha. Optimal reciprocal collision avoidance for multi-agent navigation. In *Proc. of the IEEE Int. Conf. Robotics and Automation*, Anchorage (AK), USA, 2010. IEEE.

[11] D. Martinez-Baselga, L. Riazuelo, and L. Montano. Improving robot navigation in crowded environments using intrinsic rewards. In *2023 IEEE Int. Conf. Robotics and Automation (ICRA)*. IEEE, 2023.

[12] M. Golchoubian, M. Ghafurian, K. Dautenhahn, and N. L. Azad. Uncertainty-aware DRL for autonomous vehicle crowd navigation in shared space. *IEEE Trans. Intelligent Vehicles*, 2024.

[13] M. Fahad, G. Yang, and Y. Guo. Learning human navigation behavior using measured human trajectories in crowded spaces. In *2020 IEEE/RSJ Int. Conf. Intelligent Robots and Systems (IROS)*. IEEE, 2020.

[14] H. Karnan, A. Nair, X. Xiao, G. Warnell, S. Pirk, A. Toshev, others, and P. Stone. Socially compliant navigation dataset (SCAND): A large-scale dataset of demonstrations for social navigation. *IEEE Robotics and Automation Letters*, 7(4):11807–11814, 2022.

[15] H. Okuda, T. Suzuki, K. Harada, S. Saigo, and S. Inoue. Quantitative driver acceptance modeling for merging car at highway junction and its application to the design of merging behavior control. *IEEE Trans. Intelligent Transportation Systems*, 22(1):329–340, 2019.

[16] K. Suzuki, T. Yamaguchi, H. Okuda, and T. Suzuki. Indication of interaction plans based on model predictive interaction control: Cooperation between AMRs and pedestrians using eHMI. In *2022 61st Annual Conf. the Society of Instrument and Control Engineers (SICE)*, pages 1232–1237. SICE, 2022.

[17] A. Kada, H. Okuda, K. Suzuki, and T. Suzuki. Pedestrian-aware control of AMRs using model predictive speed control minimizing pedestrian hesitation. *J. the Robotics Society of Japan*, 2025. To appear.

[18] Y. Gao and C.-M. Huang. Evaluation of socially-aware robot navigation. *Frontiers in Robotics and AI*, 8:721317, 2022.